JOURNAL OF CATALYSIS 61, 336–347 (1980)

Application of Electron-Stimulated Desorption Method for Studies of Coadsorption Process on a Platinum Foil Surface

M. J. DRINKWINE, R. DUŚ,[1] AND D. LICHTMAN

Physics Department and Laboratory for Surface Studies, University of Wisconsin–Milwaukee, Milwaukee, Wisconsin 53201

Received January 15, 1979; revised July 24, 1979

Using a common purity Pt foil, the character of adspecies adsorbed from the residual gases in a stainless-steel UHV system was studied by the electron-stimulated desorption (ESD) method. Hydrogen adatoms and dissociatively adsorbed water vapor were found as a deposit from the gas phase. The alkali metal ions, Na^+ and K^+, were readily observed by secondary ion mass spectrometry even after sputter cleaning the sample. It is suggested that alkali metal impurities could be the active sites on the Pt surface for dissociative adsorption of water. The fluorine observed on the Pt surface was thought to be a result of surface segregation of fluorine bulk impurities, with the standard enthalpy of segregation being 1600 cal/mole. A correlation between ESD of fluorine and an increase in ESD active surface hydrogen was observed. It is concluded that surface sites released by fluorine desorption are particularly active for hydrogen adsorption. Also, ESD parameters, such as total cross section, ion energy distributions, and the ion yield dependence on electron beam energy, were measured for various adspecies observed on the Pt foil.

INTRODUCTION

The aim of this work was to study the influence of electron bombardment (by means of electron-stimulated desorption (ESD)) and temperature on the adsorption phenomena that occur on a Pt foil surface exposed to the residual gases in a UHV stainless-steel system. Only a few papers concerning ESD studies on Pt have been reported up to now. Huber and Rettinghouse (*1, 2*) investigated the ESD process using a Pt sample exposed to the gases H_2, O_2, CO, and H_2O. For H_2 adsorbed on Pt, strong H^+ ESD signals were observed. They observed ESD of small amounts of CO^+, but no O^+, for CO adsorbed on Pt. Coadsorption of CO and H_2 reduced the hydrogen ESD signal considerably—probably due to competitive adsorption. Investigating a Pt–Ir (5%) sample using a high current density electron beam (10^{-4} A/cm^2) they measured the total cross section for ESD of hydrogen to be 2×10^{-16} cm^2. Similar measurements on a Pt sample produced values ranging from about 5×10^{-17} to 1×10^{-15} cm^2. Because of the presence of O^+ and OH^+ ESD signals, they suggested that H_2O was dissociatively adsorbed on their Pt–Ir sample. By means of ESD and thermal desorption Baldwin and Hudson (*3*) studied a Pt(111) surface exposed to H_2 and CO. Their results were contradictory to those of Huber and Rettinghouse in that they observed strong O^+ ESD signals and no CO^+ when CO was adsorbed on their sample. This behavior is the normal behavior for CO adsorbed on most metals. Using 1.5-keV electrons Lambert and Comrie (*4*) studied ESD of CO on Pt(111) indirectly by means of Auger spectroscopy. They found that oxygen was the main desorption product. They also concluded, as have others (*5*), that secondary electrons, returning through the adsorbed layer, play a significant role in the ESD process.

In our study we have concentrated on ESD of fluorine and hydrogen from Pt foil. This was done because under the condi-

[1] Visiting Professor from Institute of Physical Chemistry, Polish Academy of Sciences, Warsaw, Poland.

0021-9517/80/020336-12$02.00/0

tions of these experiments fluorine and hydrogen produced the predominant ESD signals. Bombarding electrons of 1000 eV were used in this study, except where otherwise noted.

ELECTRON STIMULATED DESORPTION

Electron-stimulated desorption (ESD) is the process whereby an electron, incident upon a surface, excites an adsorbed species to a repulsive state from which it subsequently desorbs. Desorbing species may be charged (positive and/or negative) or uncharged (ground state or excited state neutrals). The technique can be used as a highly surface-sensitive probe for species which are active to this process; in particular it has been used to study many systems in which hydrogen and oxygen are important surface species. Because of the difficulty involved in analyzing and detecting small numbers of neutral particles, the charged species (positive and/or negative ions) are most often the desorption products that are studied. In this study we analyze and detect only the positively charged desorbing ions.

For the reader unfamiliar with the ESD process and analysis technique and desiring additional information we refer to the list of review articles (*i–ix*) at the end of the standard reference list.

EXPERIMENTAL

A previously described (*5*), highly sensitive, ESD detection system was used in this study. A 6-in. 60° magnetic sector mass spectrometer served as the ion analyzer. With this system we are able to obtain information such as: (1) total cross sector (Q_T) for ESD, (2) ion energy distribution (IED) for ESD species, and (3) ESD ion yields vs bombarding electron energy. Secondary ion mass spectrometery (SIMS) is also an available technique. Because of the versatility and stability of the ESD system, long-term bombardment studies could be performed with minimal variation in the experimental parameters.

Pressures of 10^{-9} to 10^{-10} Torr (1 Torr = 133.3 Pa) were routinely achieved in this ion-getter pumped UHV system. A second magnetic sector mass spectrometer was used to monitor gas-phase composition during the experiments. Generally, the main components of the residual gas were H_2 and H_2O, with some CO, CO_2, and CH_4. Small amounts of other hydrocarbons were also present. Reagent-grade gases (e.g., H_2, O_2, Xe) could be introduced into the system at specified pressures via an automatic pressure controller.

The target used was made of common purity (99.9%) Pt foil. Before ESD measurements were begun, the Pt sample was sputtered (Xe^+ bombardment) and annealed (700 K at 10^{-9} Torr).

Because the ion gun–sample arrangement is set up primarily for the purpose of performing static SIMS, sputter cleaning is not highly effective when restricted to reasonable duration of ion bombardment. SIMS data indicate that surface impurity concentrations were still relatively high after the sputtering process. These impurities may be, in large part, responsible for much of the observed results reported in the following sections. However, for our purposes, this is somewhat desirable because our primary aim is to study practical surfaces such as those which may exist under production situations or in other real applications (*5*). In our ESD studies, electron beam current densities of $\leq 5 \times 10^{-6}$ A/cm^2 were used in order to minimize sample heating by the electron beam.

RESULTS AND DISCUSSION

A. *SIMS Spectra*

After the Pt foil had been partially cleaned by Xe^+ bombardment, a SIMS spectrum was obtained (Fig. 1). Na^+, K^+, and Ca^+ correspond to the largest peaks. These elements are only present on the surface in trace quantities (i.e., $\sim \leq 10^{+12}$ atoms/cm^2), but because of their very high secondary ion sensitivity (5, 6), they

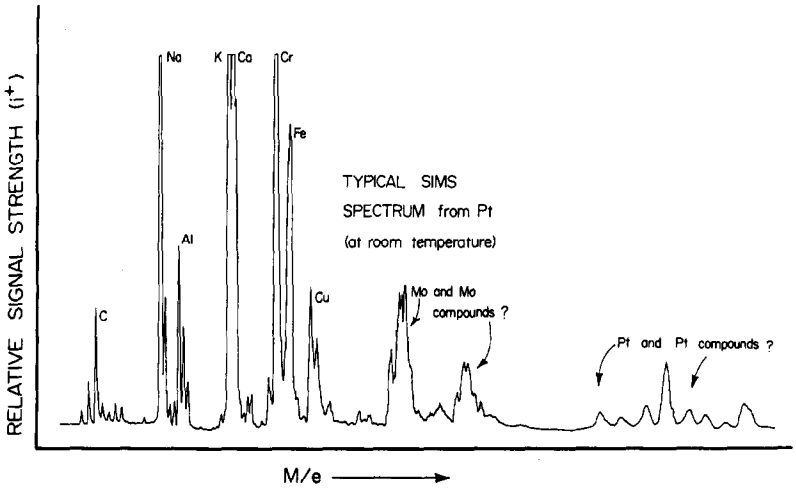

FIG. 1. SIMS spectrum from Pt foil at room temperature, using 1000-eV Xe^+ ions. The presence of Fe, Cr, and Mo ions is probably due to interaction of part of the ion beam with stainless-steel sample holder.

produce the largest peaks in the SIMS spectrum. It has been suggested by Ford and Lichtman (7) that one possible source of alkali metal impurities on surfaces may be a result of deposition of alkali halides in the form of aerosols from the atmosphere. In our opinion, this seems a likely source (rather than bulk impurities) in this case.

At this sensitivity fluorine is not observed in the SIMS spectrum. Although fluorine has relatively low secondary ion sensitivity as a positive ion, this result would still indicate that the fluorine impurity concentration is low.

Part of the ion beam impinged upon the 304 stainless-steel sample holder; this explains the presence of Fe, Cr, and Ni peaks in this SIMS spectrum. This is not a problem for the ESD studies; the electron beam is directed and focused so that it hits only the sample. The source of the Mo and Cu, which are seen in the SIMS spectrum, is not known at this time.

B. ESD Spectra and Equilibrium Studies

An ESD spectrum, obtained from the Pt foil at 298 K, is shown in Fig. 2. Fluorine and hydrogen produce the predominant peaks, with smaller peaks corresponding to oxygen, chlorine, and OH. (Although the fluorine signal is quite large it should be realized that the cross section for production of F^+ by ESD is very large; hence, these large F^+ ESD signals still represent very low fluorine concentrations at the surface—perhaps $\leq 10^{-2}$ to 10^{-3} monolayer). In order to obtain temperature-dependent equilibrium ESD data, ESD spectra were obtained with the Pt sample at a variety of temperatures in the range 300–700 K. To illustrate, spectra taken at 298, 363, and 580 K are shown in Fig. 2. Prior to electron bombardment, the Pt sample was maintained at the temperature of interest for 15–20 hr. The graph in Fig. 3 is a summary of the whole set of these experiments. One can see that the equilibrium concentration of fluorine on the surface (as determined by ESD) increases with sample temperature. However, the population of H adatoms which are active to ESD decreases with increasing temperature. Because hydrogen adsorption on Pt is an exothermic reaction with an enthalpy of 24,700 cal/mole at low coverage (*8*), this observed temperature dependence for the H^+ ESD signal should be expected. The decrease in the H^+ signal due to the incorporation of H adatoms into the bulk probably can be neglected because

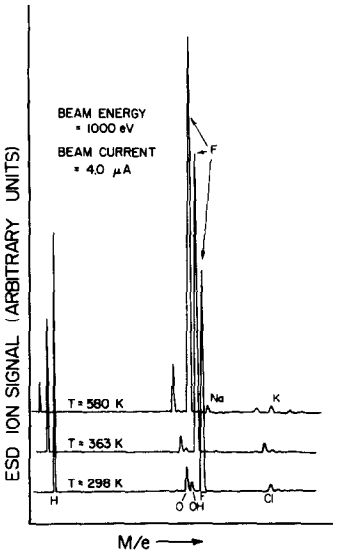

FIG. 2. ESD spectra from Pt foil, at various temperatures, having adsorbate species concentration on the surface in equilibrium with their concentration in the gas phase and in the bulk of metal. The spectra are shifted in the graph with respect to each other in order to show peak height dependences on the temperature. All spectra were obtained using electron beam of energy 1000 eV and current density of $4.5 \cdot 10^{-6}$ A/cm^2.

of the very small solubility of hydrogen in Pt.

Fluorine was absent from the gas phase; consequently, the most likely sources are platinum bulk impurities or impurities present on either the Pt surface or at the surface of the stainless-steel sample holder. (Another possible source might be the hot filament in the electron gun (*9*). This seems unlikely in this case because an "off-axis" (*5*) gun was used in these studies.) By moving the electron beam we could check for fluorine concentration gradients across the Pt sample. Within experimental error, no concentration gradient was observed between the center of the target and its edge. This suggests that the increase in the equilibrium F^+ ESD signal with temperature is due to surface segregation of fluorine from bulk impurities rather than from surface diffusion of fluorine adspecies from the stainless-steel sample holder to the sample.

As long as surface segregation is not too highly pronounced, the above suggestion would indicate that, even for a low fluorine impurity bulk concentration, the number of fluorine atoms in the bulk (N_B^F) is much greater than the number of fluorine atoms at the surface (N_S^F) for samples which are very thick in comparison to atomic spacings. We can then write

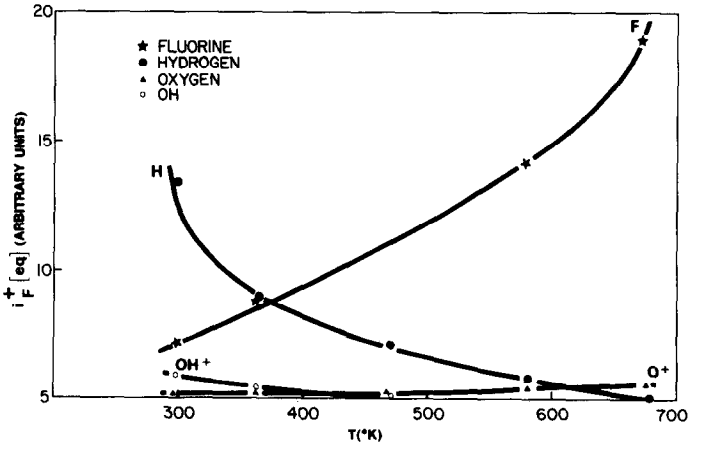

FIG. 3. ESD ion signals as a function of temperature. The concentration of adsorbate species on the surface had come to equilibrium with their concentration in the gas and in the bulk of the metal before the data were obtained.

$$\frac{N_S^F}{N_B^F} = C \exp\left[\frac{-\Delta H}{RT}\right] \simeq \frac{N_S^F}{N_T^F}, \quad (1)$$

where

ΔH is the standard enthalpy for a mole of fluorine atoms going from the bulk to the surface,
C is a constant, and
N_T^F is the total number of fluorine atoms in the sample.

For a very low bombarding electron beam current density, N_T^F is very nearly constant with time; thus it follows from Eq. (1) that

$$N_S^F \simeq k_1 \exp\left(\frac{-\Delta H}{RT}\right). \quad (2)$$

If the ionic cross section (σ^+) for ESD of F^+ does not depend on temperature, it can be shown (*10*) that the detected F^+ ion current (i_F^+) is directly proportional to the fluorine coverage

$$i_F^+(T) = i_e K \sigma^+ N_S^F(T), \quad (3)$$

where

i_e = bombarding electron current, and
K = transmission of ESD analyzer.

Using Eq. (2), this can be rewritten as

$$i_F^+(T) = k_2 \exp\left(\frac{-\Delta H}{RT}\right), \quad (4)$$

where

$$k_2 = k_1 \cdot i_e K \sigma^+.$$

In Figure 4 we show data plotted as $\ln(i_F^+)$ vs $1/T$. From these data and Eq. (4), we estimate the standard enthalpy of fluorine segregation on Pt foil to be $\simeq 1600$ cal/mole.

In our investigation we observed an O^+ and OH^+ ESD signal—presumably from adsorbed H_2O—at H_2O partial pressures of $\leq 10^{-9}$ Torr. We also observed an increase in the O^+ signal and a decrease in the OH^+ ESD signal with increasing sample temperature (Fig. 3). It has been reported (*11*) that, at room temperature or higher and H_2O partial pressures of $<10^{-4}$ Torr, H_2O does not adsorb onto clean Pt surfaces. The contradiction which our data present can be explained if the water is adsorbed onto alkali metal impurity sites or other impurities present on our Pt sample (see SIMS results). If this were the case one would expect the water to be dissociatively adsorbed. This conclusion is further substan-

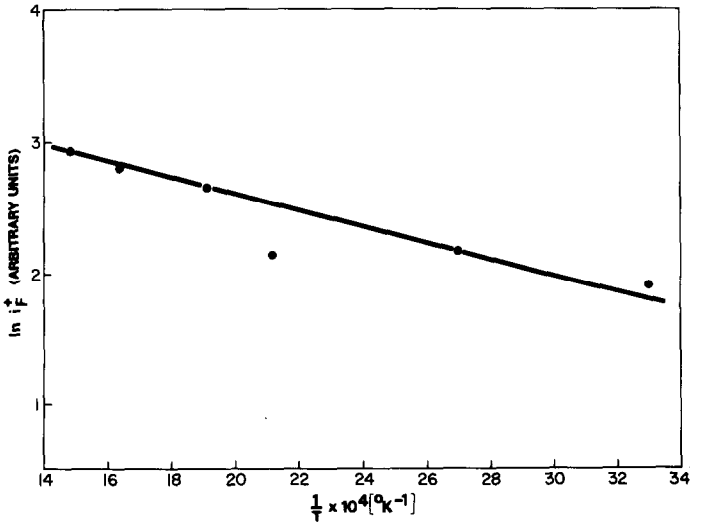

FIG. 4. A plot of the F^+ ESD data from Fig. 3 as $\ln i_F^+$ vs $1/T$. From the slope of the line the standard enthalpy of surface segregation of fluorine in Pt is calculated to be $\Delta H = 1600$ cal/mole.

tiated by the fact that no definite ESD H_2O^+ signals were observed. (It is our opinion that nondissociatively adsorbed H_2O would be bound with the oxygen atom near the surface; hence, in this case, if OH^+ ESD signals are observed, we would also expect to observe H_2O^+ ESD signals.) The behavior of the O^+ and OH^+ signals with increasing temperature is also consistent with dissociative adsorption of H_2O at alkali impurity sites: at higher temperatures the dissociation of H_2O at alkali impurities can lead to the complete dehydrogenation of H_2O adspecies resulting in the formation of oxygen adatoms. (We should note, for future reference, that because of the presence of the OH^+ signal, it is very likely that part of our H^+ signal is due to ESD of H^+ from dissociatively adsorbed H_2O.) As mentioned earlier, Huber and Rettinghouse (*1, 2*) also observed O^+ and OH^+ ESD signals. In view of our findings and other work (*11*) it is very likely that their sample also contained surface impurities which served as active sites for dissociative adsorption of H_2O.

When the system was backfilled with H_2 gas to a pressure of $\sim 5 \times 10^{-6}$ Torr, there was no change in the O^+ or OH^+ ESD signals. This would further indicate that the OH adspecies were formed by dissociative adsorption of water—not by the reaction of hydrogen with oxygen adatoms. The possible existence of some inactive oxygen adatoms on Pt (and even Pd) surfaces has been previously reported (*10, 11*).

C. *Nonequilibrium ESD Studies*

When the bombarding electron beam current density (J_e) was increased to values $\geq 10^{-6}$ A/cm^2, decay of the F^+ ESD signal was readily observed. By measuring the rate of signal decay, the total cross section for ESD of fluorine (Q_F) can be obtained according to the well-known equation (*10*)

$$i_F^+(t) = i_F^+(0) \exp\left[\frac{-J_e Q_F t}{e}\right] \qquad (5)$$

where

$i_F^+(t)$ is the detected F^+ signal after time t of electron bombardment,
$i_F^+(0)$ is the signal at the beginning of bombardment, and
e is the electronic charge.

During electron bombardment for periods of $\sim$15 min using a beam current density of 5×10^{-6} A/cm^2 we observed a decay in F^+ signal (see Fig. 7) which corresponded to $Q_F = 1 \times 10^{-17}$ cm^2. The uncertainty in this value is approximately 50%. It has been found (*5*) that the total cross section for ESD of fluorine from "as is" 304 stainless steel is also $\sim 1 \times 10^{-17}$ cm^2. Furthermore, Q_F for ESD of fluorine from CCl_2F_2 adsorbed on polycrystalline W has been found to be 4×10^{-18} cm^2 (*13*)—very nearly the same as that found here. The available data would tend to indicate, at this time, that the cross section for ESD of fluorine is relatively substrate independent—at least for systems in which fluorine is readily observed.

When the target was bombarded for an extended time ($\sim$5 hr) using a high beam current density ($J_e = 1 \times 10^{-5}$ A/cm^2), the observed behavior of the F^+ signal was not (just) as predicted by Eq. (5). Prior to the collection of these data the sample had been allowed to come to equilibrium for 15 hr at 298 K with no electron bombardment. In Fig. 5, curve A, we show the observed behavior of the F^+ ESD signal; curve B shows the expected behavior calculated according to Eq. (5) and using $Q_F = 1 \times 10^{-17}$ cm^2. A comparison of these two curves leads to the conclusion that there existed a source of fluorine which would repopulate the surface. We believe this source to be fluorine diffusion from the bulk. This same claim was made earlier on the basis of our equilibrium ESD studies. We can now further substantiate this claim in the following discussion.

The difference between curves A and B was determined and integrated. This gave a value proportional to the amount of fluorine

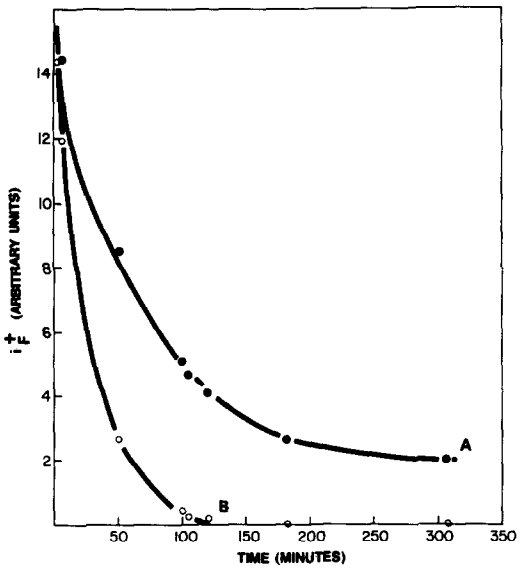

FIG. 5. Curve A shows the observed behavior of the F^+ ESD ion signal as a function of time, at room temperature, using an electron current density of $1 \cdot 10^{-5}$ A/cm^{-5}. Curve B shows the expected behavior which should have been observed in the absence of any repopulation source, assuming $Q_F = 1 \cdot 10^{-17}$ cm^2.

repopulation vs time. Plotting this value as a function of the square root of time ($t^{1/2}$), we obtained the graph presented in Fig. 6. For the case where the bombarding electron beam is dense enough, the F^+ ESD ion current will be controlled by the diffusion process (if there are no other sources of fluorine) and consequently described by

$$i_F^+(t) = B\, t^{1/2}, \qquad (6)$$

where B is a constant independent of time. Indeed, in the results shown in Fig. 6, for $t^{1/2} > 11$, one can see that Eq. (6) is valid. For $t^{1/2} < 11$, the surface concentration is controlled by both the ESD process and diffusion. This behavior agrees with the expectation that, if there were no diffusion, the ESD F^+ signal would be nearly zero (Fig. 5, curve B) at $t^{1/2} \geq 11$. When taking this diffusion effect into account, our calculated value for Q_F will not be changed by more than the original experimental uncertainty.

It might be possible for the preceding results to be explained on the basis of "uncovering" fluorine during the bombardment rather than a diffusion process. However, for this to be the case more assumptions would have to be made about the special behavior of the overlayer than were made in the previous discussion. We believe that diffusion of fluorine is the more probable phenomenon. In the course of obtaining data for the determination of Q_F we observed that the decrease of F^+ signal was accompanied by an increase in the H^+ ESD ion signal. At room temperature the rate of H^+ signal increase was very nearly the same as the rate of F^+ decrease, as shown in Fig. 7. This behavior suggests the possible explanation that surface sites released by fluorine desorption were particularly active to hydrogen adsorption.

The number of surface sites, $N^*(t)$, "released" due to fluorine desorption can be estimated by applying Eq (3) to the data of Figure 7:

$$N^*(t) = N_0^F \left| 1 - \frac{i_F^+(t)}{i_F^+(0)} \right|, \qquad (7)$$

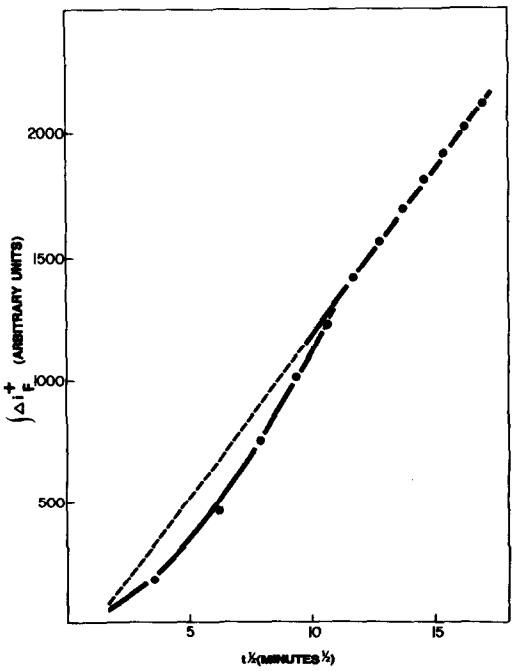

FIG. 6. The "integrated difference" between curves A and B from Fig. 5 vs $t^{1/2}$ for F^+. As it was expected for $t^{1/2} > 11$ the diffusion equation (6) holds.

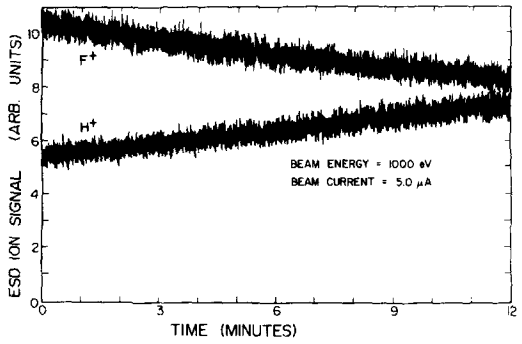

FIG. 7. It was observed that while the F^+ decayed during electron bombardment, the H^+ signal increased. Data obtained at electron current density $5 \cdot 10^{-6}$ A/cm^2.

where N_0^F is the number of sites occupied by fluorine at the beginning of the electron bombardment. We can expect that readsorption of hydrogen will be very nearly complete during the electron bombardment because:

(1) the enthalpy of hydrogen adsorption is high (~25 kcal/mole) (*8*),
(2) the target was kept at room temperature in these experiments,
(3) the hydrogen partial pressure was of the order 10^{-9} Torr, and
(4) the data were acquired over a relatively long period of time (15 min) using an electron beam current density that was rather low (~10^{-6} A/cm^2).

If we assume that hydrogen adsorbs on all the sites, $N^*(t)$, "released" by desorption of fluorine, we can write:

$$N^H(t) = N_0^H + N^*(t), \qquad (8)$$

where $N^H(t)$ is the hydrogen population at time t, and N_0^H is the hydrogen population at the beginning of the electron bombardment. Combining Eq. (3), (7), and (8), we can write

$$\frac{i_H^+(t) - i_H^+(0)}{i_F^+(0) - i_F^+(t)} = \frac{\sigma_H^+}{\sigma_F^+}. \qquad (9)$$

According to this model and assuming that σ_F^+ is known, the ionic cross section (σ_H^+) for ESD of hydrogen from Pt foil can be calculated using the data presented in Fig. 7.

In work done in our laboratory (*13*, *14*) there is a strong indication that the ESD cross sections for desorption of fluorine are relatively substrate independent. Furthermore, it is very likely that $\sigma_F^+ \cong Q_F$. It has been very carefully determined (*13*) that Q_F for ESD of fluorine from CCl_2F_2 adsorbed on polycrystalline tungsten is 4×10^{-18} cm^2. Therefore, let us use the above observations and assume that the ionic cross section (σ_F^+) for ESD of fluorine from our Pt sample is 4×10^{-18} cm^2. Then, using the data presented in Fig. 7, we calculate (according to Eq. (9)) σ_H^+ to be $\sim 3 \times 10^{-18}$ cm^2 for ESD of H^+ from Pt foil. This value is approximately 100 times smaller than the Q_H measured by Huber and Rettinghouse (*2*) for ESD of hydrogen from Pt. This difference of a factor of 100 should be expected when comparing Q_H to σ_H^+; a ratio of $Q_H/\sigma_H^+ \cong 100$ has been observed in nearly all studies of hydrogen desorbed by ESD from metal surfaces.

It should be emphasized that Eq. (9) is valid only under the assumptions that: (1) thermal desorption of hydrogen is negligible, and (2) hydrogen readsorption during electron bombardment is complete. When the bombarding electron beam current density was increased above what it was for the previous results by 10 times, so that condition 2 no longer holds, we observed that the hydrogen signal did *not* behave as the inverse of the change in the F^+ signal.

Our proposed mechanism is further substantiated by the fact that, for low enough beam current densities, Eq. (9) is satisfied for all times t. This behavior is shown in Fig. 8. Also, we have an independent check on σ_H^+ as indicated in Eq. (3). The transmission coefficient, K, of our analyzer was measured to be $\sim 6 \times 10^{-3}$. If we estimate the hydrogen coverage on our Pt sample to be 0.001–0.01 of a monolayer (a reasonable estimate) we calculate σ_H^+ to be $\sim 10^{-18}$ cm^2. This is in rough agreement with our results obtained using Eq. (9).

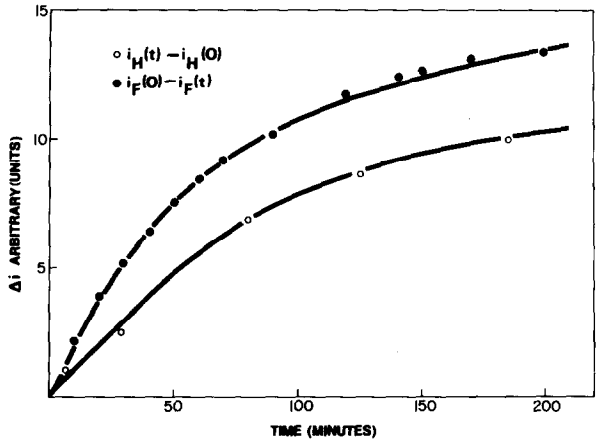

FIG. 8. The ratio of the difference signals

$$\left(\frac{i_H^+(t) - i_H^+(0)}{i_F^+(0) - i_F^+(t)}\right)$$

continuously behaves according to Eq. [9] with $\sigma_H^+/\sigma_F^+ \sim 0.75$ for long bombardment time. This behavior is consistent with our interpretation. The electron beam density was $4.5 \cdot 10^{-6}$ A/cm^2.

We observe that the chlorine and oxygen ESD signals descreased slightly during electron bombardment. Total cross sections for ESD of these species were determined (according to Eq. (5) to be

$$Q_{Cl} = 5 \pm 3 \times 10^{-18}\ \text{cm}^2,$$

$$Q_O = 2 \pm 1 \times 10^{-18}\ \text{cm}^2$$

D. Electron-Assisted Desorption of Alkali Ions

During the course of our investigation we observed large thermal desorption ion signals corresponding to K^+ ions—even at moderate temperatures (i.e., 700 K), as shown in Fig. 9A. Thermal desorption of Na^+ was also observed, but not in significant quantities. Surface thermal ionization is a well-known phenomenon (*16, 17*) so these observations are not surprising considering our SIMS results (Fig. 1) which indicate the presence of Na and K on the Pt surface.

When the temperature of the Pt foil was lowered to 580 K, thermal desorption of K^+ ions was not detectable (Fig. 9B). However, with the sample still at 580 K, we observed small signals corresponding to Na^+ and K^+ ions when the electron beam was turned on (Fig. 9C). At lower temperatures this effect was not observed. For the beam power densities used here, the maximum increase in sample temperature was calculated (*18*) to be no more than 10 K. Hence, it is unlikely that electron beam heating of the sample was responsible for this observed behavior. It is more likely that we observed ESD of thermally excited

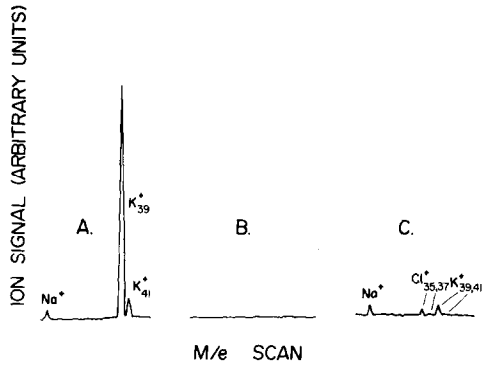

FIG. 9. At 700 K the Pt target shows strong K^+ thermal desorption. At 580 K, K^+ ions are observed only with the electron beam bombarding the target. (A) e^- beam off, target temperature = 700 K; (B) e^- beam off, target temperature = 580 K, sensitivity = ×20; (c) e^- beam on, target temperature = 580 K; sensitivity = ×20.

alkali metal adatoms. Electron-induced desorption of alkali metal ions has been observed before (*19*), but more work is needed to adequately explain this behavior.

E. Ion Energy Distributions of Ions Desorbed by ESD

The IEDs for H^+, F^+, O^+, OH^+, and Cl^+ ESD ions were measured at various target temperatures. It was found that, within the range 300–700 K, temperature has little effect on the IEDs. The normalized results obtained at 298 K are presented in Fig. 10. The fact that the H^+ and F^+ IEDs are similar might be correlated with our hypothesis that hydrogen and fluorine are adsorbed at similar surface sites. This supposition is supported by the observation that: (1) species which we believe to be adsorbed at sites dissimilar to hydrogen and fluorine adsorption sites (namely, O, OH, and Cl) do not have IEDs like H^+ or F^+, and

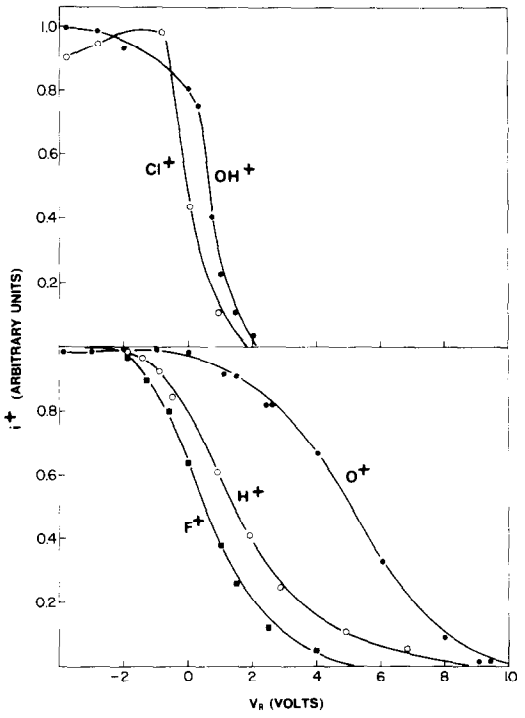

FIG. 10. Normalized ESD ion signal vs retarding potential applied to analyzer entrance grids. The ion energy distributions (IED) can be obtained by differentiation.

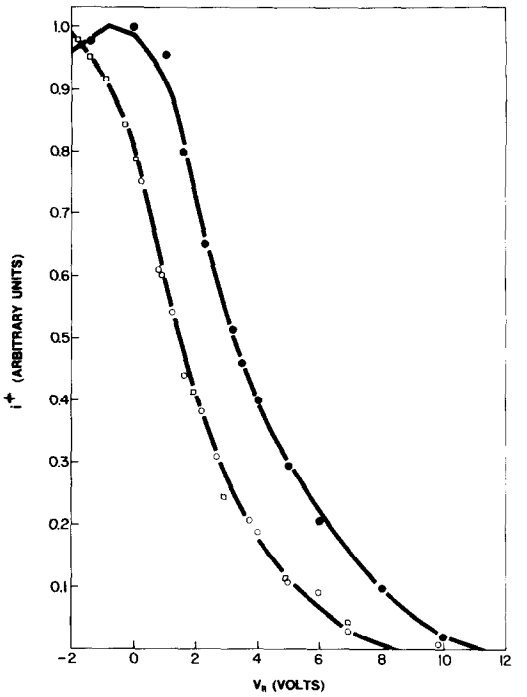

FIG. 11. The bombardment of the Pt target with Xe^+ ions shifted the IED of hydrogen ions. IED of hydrogen ions before XE^+ bombardment is indicated by open dots, and IED after Xe^+ bombardment by black dots. Annealing of the Pt foil caused return to IED of previous shape (squares).

(2) the H^+ IED can be significantly changed by bombardment of the Pt foil with Xe^+ ions. (This bombardment probably changes the character of the surface sites accessible for hydrogen adsorption. Annealing the Pt foil caused the previously observed H^+ IED to return. See Fig. 11.)

F. ESD Ion Yields vs Bombarding Electron Energy

The ESD ion yield for H^+, F^+, and O^+ was measured as a function of bombarding electron energy (in the inverval 50–3000 eV), and sample temperature (in the range 300–700 K). Results similar to those obtained using a stainless-steel substrate (*5*) were observed (Fig. 12). The maximum H^+ and F^+ yield was measured for an electron energy of ~150 eV. The O^+ yield was a maximum for electron energies near 250

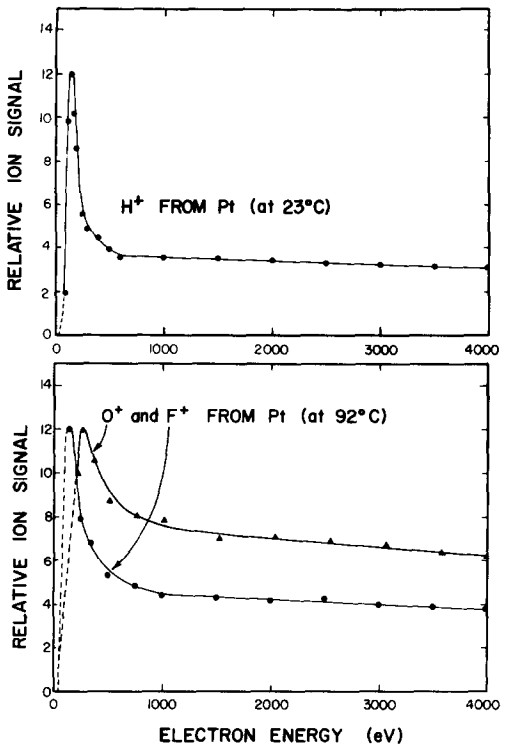

FIG. 12. ESD ion yields vs bombarding electron energy. The curves have been normalized so that the maximum has the same height in each case.

eV. The H^+ yield vs electron energy showed a small temperature dependence with the maximum yield shifting to ~250 eV at a target temperature of 580 K. The measurements for F^+ and O^+ showed little variation as a function of temperature.

SUMMARY

We have investigated ESD of various desorption species from Pt foil as a function of several different parameters.

(1) H^+, F^+, O^+, OH^+, and Cl^+ were the principal ESD species.

(2) The source of fluorine on the surface was very likely surface segregation of bulk impurity fluorine. The standard enthalpy of fluorine surface segregation was calculated to be ~1600 cal/mole.

(3) For our Pt sample, water is probably adsorbed dissociatively at alkali metal or other metal impurity sites.

(4) The total cross section for ESD of fluorine was determined to be $\sim 1 \times 10^{-17}$ cm^2. This is very nearly the same as that determined for ESD of fluorine from stainless steel (*5*), polycrystalline tungsten (*13*), and niobium foil (*20*).

(5) Our ESD data are consistent with a mechanism in which hydrogen is adsorbed at sites which have been "freed" by ESD of fluorine. There may be adsorption of hydrogen elsewhere, but the adsorbed hydrogen which is active to ESD is apparently associated with these "freed" sites. The corresponding ionic cross section for ESD of this hydrogen is $\sigma_{H^+} = 3 \times 10^{-18}$ cm^2.

(6) Thermal desorption of alkali ions was observed. We also observed what we call "electron-assisted desorption" of alkali ions.

(7) The ion energy distributions of ESD ions were measured. The IEDs were relatively insensitive to temperature changes over the range 300–700 K. Our results indicate that the IED may be sensitive to the particular type of adsorption site as well as the type of desorbing species. In this case the adsorption site is probably characteristic of a metal atom impurity.

(8) The relative ESD cross section vs the energy of the bombarding electrons is very similar to that reported for a stainless-steel substrate (*5*). The overall behavior is similar to gas-phase ionization cross sections, but somewhat broadened. There are variations for different desorbing species, but these variations are minor, as in the case of gas-phase ionization of different molecules. As in previous work (*4, 5*), these results indicate that secondary electrons passing through the adsorbed layer as they leave the surface produce significant desorption as compared to the primary beam.

It should be emphasized that the sample used in this investigation was contaminated with various surface impurities. Consequently, it is difficult to compare our results to results of others working with an ultra-clean Pt surface. However, surfaces encountered in real and practical applications are seldom without high levels of contamination. The fact that a solvent-cleaned Pt foil (nominally 99.9% pure) shows such a high level of surface impurities and a high reactivity to ESD is important to keep in mind when dealing with Pt in real applications—especially in catalytic reactors where conditions are quite different from those encountered in the laboratory under ultra high vacuum, using atomically clean surfaces.

ACKNOWLEDGMENTS

We would like to gratefully acknowledge the support of ERDA, Materials and Radiation Effects Branch, Division of Magnetic Fusion Energy, Contract EY-76-S-02-2425. We acknowledge the support for one of us (R.D.) from the National Science Foundation, Grant INT-7522132.

REFERENCES

1. Huber, W. K., and Rettinghouse, G., *J. Vac. Sci. Technol.* **6**, 89, (1969).
2. Huber, W. K., and Rettinghouse, G., *J. Vac. Sci. Technol.* **7**, 289, (1970).
3. Baldwin, V. H., and Hudson, J. B., *J. Vac. Sci. Technol.* **8**, 49, (1971).
4. Lambert, R. M., and Comrie, C. M., *Surface Sci.* **38**, 197, (1973).
5. Drinkwine, M. J., and Lichtman, D., *J. Vac. Sci. Technol.* **15**, 74, (1978).
6. Benninghoven, A., *Surface Sci.* **53**, 596, (1975).
7. Ford, R. R., and Lichtman, D., *J. Appl. Phys.* **40**, 5088, (1969).
8. Norton, D. R., and Richards, P. J., *Surface Sci.* **44**, 129, (1974).
9. Wiedmann, L., Ganschow, O., and Benninghoven, A., *J. Electron Spectrosc. Relat. Phenom.* **13**, 243, (1978).
10. Madey, T. E., and Yates, J. T., Jr., *J. Vac. Sci. Technol.* **8**, (1971) 525.
11. Duś, R., and Tompkins, F. C., *Proc. Roy, Soc. (A)* **343**, 477, (1975).
12. Duś, R., and Lisowski, W., *Surface Sci.* **59**, 141, (1976).
13. Vica de Moraes, M. A., Ph.D. thesis, University of Wisconsin–Milwaukee, 1978.
14. Drinkwine, M. J., Ph.D. thesis, University of Wisconsin–Milwaukee, 1977.
15. Drinkwine, M. J., and Lichtman, D., *Progr. Surface Sci.* **8**, 123, (1977).
16. Datz, S., and Taylor, E. H., *J. Chem. Phys.* **25**, 395, (1956).
17. Lichtman, D., *J. Vac. Sci. Technol.* **2**, 91, (1965).
18. Fabel, G. W., Cox, S. M., and Lichtman, D., *Surface Sci.* **40**, 571, (1973).
19. Lichtman, D., and McQuistan, R. B., *Progr. Nuclear Energy Ser. 9* **4**, Pt. 2 (1965).
20. Duś, R., Drinkwine, M. J., and Lichtman, D., (To be submitted).

ESD REVIEW ARTICLES

i. Lichtman, D., and McQuistan, R. B., *Progr. Nucl. Energy Ser. 9* **4**, Pt. 2, 95 (1965).
ii. Redhead, P. A., *J. Vac. Sci. Technol.* **7**, 182 (1970).
iii. Madey, T. E., and Yates, J. T., Jr., *J. Vac. Sci. Technol.* **8**, 525 (1971).
iv. Leck, J. H., and Stimpson, B. P., *J. Vac. Sci. Technol.* **9**, 293 (1972).
v. Ageev, V. N., and Ionov, N. I., *Progr. Surface Sci.* **5**, 1 (1974).
vi. Gomer, R., *Solid State Phys.* **30**, 93 (1975).
vii. Menzel, D., *Surface Sci.* **47**, 370 (1975).
viii. Drinkwine, M. J., and Lichtman, D., *Progr. Surface Sci.* **8**, 123 (1977).
ix. Madey, T. E., and Yates, J. T., Jr., *Surface Sci.* **63**, 203 (1977).